

Dipyrimidine Amines: A Novel Class of Chemokine Receptor Type 4 Antagonists with High Specificity

Aizhi Zhu,^{†,‡} Weiqiang Zhan,^{‡,‡} Zhongxing Liang,[†] Younghyun Yoon,[†] Hua Yang,[§] Hans E. Grossniklaus,[§] Jianguo Xu,^{||} Mauricio Rojas,^{||} Mark Lockwood,[‡] James P. Snyder,^{*,‡} Dennis C. Liotta,^{*,‡} and Hyunsuk Shim^{*,†,⊥}

[†]Department of Radiology, [‡]Department of Chemistry, [§]Department of Ophthalmology, ^{||}Division of Pulmonary, Department of Medicine, and [⊥]Winship Cancer Institute, Emory University, Atlanta, Georgia 30322, United States. [#]These authors contributed equally to this work.

Received June 24, 2010

The C-X-C chemokine receptor type 4 (CXCR4)/stromal cell derived factor-1 (SDF-1 or CXCL12) interaction and the resulting cell signaling cascade play a key role in metastasis and inflammation. On the basis of the previously published CXCR4 antagonist **5** (WZ811), a series of novel nonpeptidic anti-CXCR4 small molecules have been designed and synthesized to improve potency. Following a structure–activity profile around **5**, more advanced compounds in the *N,N'*-(1, 4-phenylenebis(methylene)) dipyrimidin-2-amines series were discovered and shown to possess higher CXCR4 binding potential and specificity than **5**. Compound **26** (508MCI) is the lead compound and exhibits subnanomolar potency in three in vitro assays including competitive binding, Matrigel invasion and $G\alpha_i$ cyclic adenosine monophosphate (cAMP) modulation signaling. Furthermore, compound **26** displays promising effects by interfering with CXCR4 function in three mouse models: paw inflammation, Matrigel plug angiogenesis, and uveal melanoma micrometastasis. These data demonstrate that dipyrimidine amines are unique CXCR4 antagonists with high potency and specificity.

Introduction

Chemokines are a superfamily of small cytokines that induce cytoskeleton rearrangements and directional migration of several cell types through their interaction with G-protein-coupled receptors.¹ These secreted proteins act in a coordinated fashion with cell-surface proteins, including integrins, to direct the specific homing of various subsets of hematopoietic cells to specific anatomical sites.^{2,3} One member of the chemokine family, stromal cell derived factor-1 (SDF-1; also named CXCL12⁴), is a chemokine that interacts specifically with C-X-C chemokine receptor type 4 (CXCR4) which was previously identified as a major coreceptor for the entry of T cell line-tropic HIV.^{4–7} The CXCL12/CXCR4 interaction was later shown to direct cellular recruitment and trafficking, and it offers a new target for indications where such processes play a key role. This interaction also

plays a central role in the locomotion and homing of metastatic cells. Therefore, interruption of this interaction may provide a means of intervening in the metastatic process.

Currently, cyclams and bicyclams represent the most thoroughly studied class of nonpeptide anti-CXCR4 molecules. However, this class of inhibitors is not ideal for long-term treatment due to cyclam's metal ion chelating property, which may result in cardiotoxicity.⁸ Two years ago, we reported the identification of a novel class of small molecule CXCR4 antagonists.⁹ In view of aspects of the molecular mechanism of the bicyclam CXCR4 antagonist **1** (AMD3100⁸), we designed a template with the general structure **2** and identified the first lead compound **3** by means of an affinity binding assay against the potent, peptidic CXCR4 antagonist **4** (TN14003¹⁰) (Figure 1). An extensive structure–activity profile around **3** indicated the central aromatic ring to be critical for high CXCR4 affinity, and a one-carbon separation between the central aromatic phenyl ring and the nitrogen of the acyclic linker is essential for high potency. These SAR features finally led to identification of compound **5** (WZ811⁹) as a potential CXCR4 antagonist that shows excellent potency in an affinity binding assay and in vitro function assays. Unfortunately, further preclinical studies suggested that compound **5** failed to exhibit any in vivo efficacy due to poor bioavailability (data not shown). We explored further reiteration of the compounds.

On the basis of the working hypothesis that the poor pharmacokinetic profile of **5** might be the result of rapid oxidative metabolism, various electron deficient moieties have been introduced to the terminal aromatic ring of **5**. The synthetic pathways employed to prepare the final compounds are depicted in Schemes 1, 2, and 3. For the primary screening, a competitive binding assay utilizing the potent, peptidic

*To whom correspondence should be addressed. For H.S.: phone, 404-778-4564; fax, 404-778-5550; E-mail, hshim@emory.edu; address, Department of Radiology, Winship Cancer Institute, Emory University, 1365C Clifton Road, NE, C5008, Atlanta, GA 30322. For D.C.L.: phone, 404-727-6602; fax, 404-727-1094; E-mail, dliotta@emory.edu; address, Department of Chemistry, Emory University, 1521 Dickey Drive, Atlanta, GA 30322. For J.P.S.: phone, 404-727-2415; fax, 404-712-8679; E-mail, jsnyder@emory.edu; address, Department of Chemistry, Emory University, 1521 Dickey Drive, Atlanta, Georgia 30322, United States.

^aAbbreviations: GPCRs, G protein-coupled receptors; CXCR4, C-X-C chemokine receptor type 4; CXCL12, C-X-C chemokine ligand 12; CCR3, C-C chemokine receptor type 3; CCR5, C-C chemokine receptor type 5; SDF-1, stromal-derived factor-1; cAMP, cyclic adenosine monophosphate; AIDS, acquired immune deficiency syndrome; HIV, human immunodeficiency virus; EC, effective concentrations; TR-FRET, time-resolved-fluorescence resonance energy transfer; TLC, thin layer chromatography; H&E, hematoxylin and eosin; CD, (2-hydroxypropyl)- β -cyclodextrin; FDA, Food and Drug Administration; PBS, phosphate buffered saline.

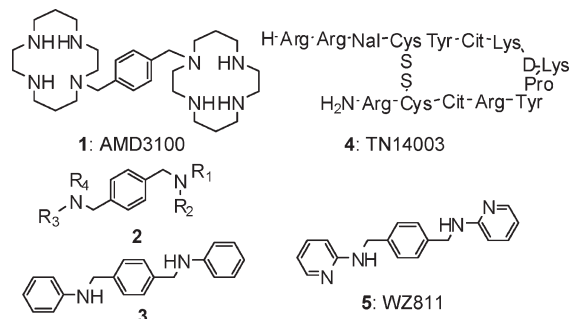
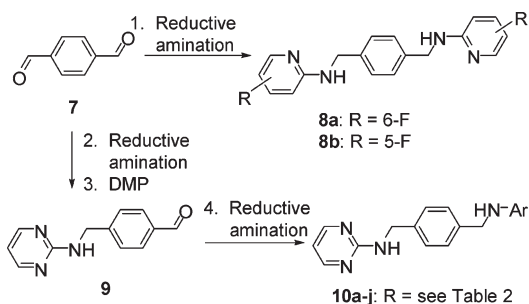


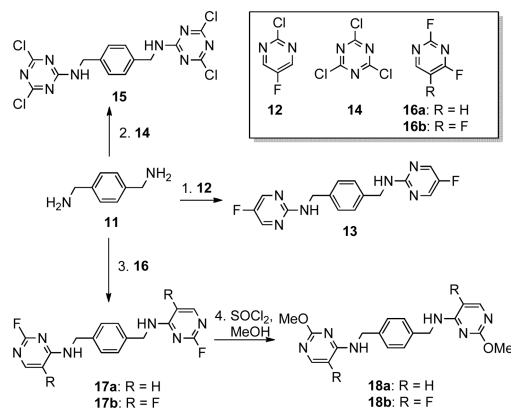
Figure 1. Structures of nonpeptidic CXCR4 antagonist **1**, potential CXCR4 antagonist template **2**, potential CXCR4 antagonist lead compound **3**, peptidic CXCR4 antagonist **4**, and potential CXCR4 antagonist **5**.

Scheme 1^a



^a Reagents and conditions: (1) 2-amino-fluoropyridines, NaBH(OAc)₃, HOAc, ClCH₂CH₂Cl, 61–64%; (2) 2-amino-pyrimidine, NaBH(OAc)₃, HOAc, ClCH₂CH₂Cl, 82%; (3) DMP, CH₂Cl₂, 94%; (4) ArNH₂, NaBH(OAc)₃, HOAc, ClCH₂CH₂Cl, 65–69%.

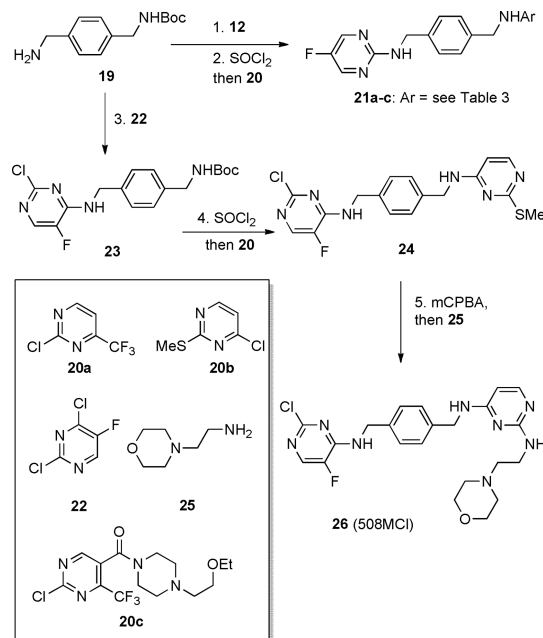
Scheme 2^a



^a Reagents and conditions: (1) **12**, Cs₂CO₃, DMF, 75%; (2) **14**, NaHCO₃, THF, 94%; (3) fluoropyrimidines (**16a–b**), DIPEA, DMF, 65–70%; (4) SOCl₂, MeOH, quant.

CXCR4 antagonist **4** was employed. Previously, we described the rationale for using this assay as our primary assay.^{9,11} In addition, two functional assays measuring cAMP modulation and Matrigel invasion were performed to determine the rank order of anti-CXCR4 efficacy of the newly designed and synthesized compounds.^{12–14} Furthermore, the in vivo effects of the selected compounds were tested in two mouse models: paw edema for inflammation and Matrigel plug for angiogenesis. Finally, the lead compound **26** (508MCl) was tested in mouse lung fibrosis and uveal melanoma micrometastasis models.

Scheme 3^a



^a Reagents and conditions: (1) **12**, DIPEA, DMF, 96%; (2) SOCl₂, then **20a–c**, DIPEA, DMF, 63–72% (2 steps); (3) **22**, DIPEA, DMF, 94%; (4) SOCl₂, MeOH, then **20b**, DIPEA, DMF, 65% (2 steps); (5) *m*CPBA, CH₂Cl₂, then **25**, dioxane, 25% (2 steps).

Results and Discussion

Chemistry. The synthesis of the target compounds is illustrated in Schemes 1–3. Compound **8a** and **8b** were prepared from the one-pot reductive amination of aldehyde **7** and fluoropyridin-2-amines in the presence of the reducing reagent NaBH(OAc)₃.¹⁵ To prepare compounds **10a–j**, aldehyde **9** was first generated by a two-step sequence from aldehyde **7**, followed by reductive amination to give the desired compounds **10a–j** (Scheme 1). As shown in Scheme 2, compound **13** was synthesized by treating amine **11** with 2-chloro-5-fluoropyrimidine **12** in good yield. Following a similar strategy, compounds **15**, **17a**, and **17b** were prepared efficiently. Subsequently, treating compound **17a/b** with SOCl₂ in methanol delivered the methoxyl-substituted analogue **18a/b** (Scheme 2). The synthesis of compounds **21a–c** starts from mono-Boc-protected amine **19**. Amine **19** was first treated with 2-chloro-5-fluoropyrimidine **12**, and the Boc was subsequently removed in the presence of SOCl₂, followed by an addition–elimination sequence to furnish the desired target compounds **21a–c** (Scheme 3). A similar synthetic strategy also efficiently delivers compounds **23** and **24**. Subsequent *m*CPBA mediated oxidation converted **24** into a mixture of 2-(methylsulfinyl)pyrimidine and 2-(methylsulfonyl)pyrimidine derivatives, which were treated with 2-morpholinoethanamine **25** without further purification to afford compound **26** in 25% yield over two steps (Scheme 3).

Primary Screening. On the basis of the behavior of **5**, we know that the central 1,4-bis-(aminomethyl)benzene group is critical for CXCR4 binding affinity. Consequently, the distal pyridinyl ring was modified in several ways. For primary compound screening, the previously reported assay was utilized.⁹ MDA-MB-231 cells were preincubated with compounds at concentrations of 1, 10, 100, and 1000 nM, following incubation with biotinylated **4** and streptavidin-conjugated rhodamine to determine the binding efficiency of

Table 1. Effects of Symmetrical Compounds As Blockers of CXCR4 Binding and Matrigel Invasion^a

Entry	Compd	Ar	TN-binding Blocking	Invasion Inhibition	
			EC (nM)	100nM	10nM
1	3		10	64%	54%
2	6		100	58%	32%
3	5		10	90%	72%
4	8a		100	85%	55%
5	8b		100	68%	45%
6	13		1	75%	75%
7	15		10	82%	61%

^a In this paper, EC (effective concentration) is defined as the concentration at which the compound blocks > 50% of **4** binding to CXCR4.

the newly synthesized chemical entities to the CXCL12 binding domain of CXCR4. The effective concentration (EC) is defined as the concentration at which the compound blocks more than 50% of **4** binding on CXCR4. Thus, the EC values of compounds meeting this criterion were determined. The Matrigel invasion assay, as the secondary functional assay, was performed for those compounds with an EC value lower than 100 nM to test whether they could block the CXCR4/CXCL12-mediated chemotaxis and invasion as utilized previously.⁹ The results of competitive binding and Matrigel invasion are summarized in Table 1. It should be noted that more electron deficient functional groups were introduced to compound **5** to maintain the symmetric chemical structure (Table 1). Pyrimidinyl compound **13** was identified as a potent CXCR4 antagonist with high CXCR4 binding affinity and efficient blocking of Matrigel invasion (> 75%) at 10 nM. With the discovery of the pyrimidinyl group as a potent pharmacophore for CXCR4 antagonists, a series of unsymmetrical compounds were designed and prepared with a pyrimidinyl ring at one terminus of the scaffold and a pyridinyl ring on the other with different functional groups. All these substances exhibited excellent antagonist activity (> 60%, Table 2) at 100 nM and > 40% at 10 nM against CXCR4/CXCL12-mediated Matrigel invasion. Furthermore, we designed and synthesized dual pyrimidinyl compounds with different functional groups such as methoxy and morpholinyl to adjust their hydrophilicity. We assumed that increased hydrophilicity could increase the compounds' binding affinity to CXCR4 (Table 3). Most of the corresponding compounds show exceptional inhibition of CXCR4 with EC values at 1 nM, except **18a**, with an EC

value at 10 nM. While these compounds also scored well in the Matrigel invasion assay with > 65% inhibition at 100 nM, **21a**, **21b**, **21c**, **17a**, **18b**, and **26** are especially effective at blocking invasion between 81% and 100%. At a concentration as low as 10 nM, **21a**, **21b**, **17a**, **18b**, and **26** inhibit invasion > 60%; **26** blocks 84% of invasion at 10 nM. Interestingly, all dipyrimidines demonstrated high potency without being significantly influenced by variable substitution.

cAMP Assay. As a GPCR, CXCR4 binds CXCL12 and activates G-protein mediated signaling through the G α_i pathway that reduces cAMP levels within cells. Therefore, we utilized the cAMP assay as the secondary functional assay as reported previously.⁹ The selection criteria for the compounds subjected to the cAMP assay was an EC \leq 10 nM binding affinity and > 50% inhibition of invasion at 10 nM. After pretreatment for 15 min at room temperature with **1** and selected compounds, the effect of CXCL12 on cAMP reduction was blocked significantly in a dose-dependent manner. Compounds **21c** with an IC₅₀ at 5.4 \pm 0.17 nM and **26** with an IC₅₀ at 0.8 \pm 0.13 nM counteracted CXCL12 function effectively at nanomolar concentrations, while **1** required nearly 1000 nM to significantly block CXCL12 function with an IC₅₀ at 695 \pm 21 nM. These compounds are almost 1000-fold more efficient in blocking the G α_i pathway than **1** (Figure 2A). Compounds **21c** and **26** are comparable to or even better than the previously reported **5** with an IC₅₀ at 1.8 \pm 0.24 nM.⁹ The specificity of **21c** and **26** to CXCR4 was tested using U87CD4 cell lines from the AIDS Consortium overexpressing the CCR3 or CCR5 chemokine receptors. These cells were stimulated by 150 ng/mL CCL5 instead of CXCL12. Figure 2B shows the cAMP assay results

Table 2. Effects of Asymmetrical Compounds As Blockers of CXCR4 Binding and Matrigel Invasion^a

Entry	Compd	Ar	TN-binding Blocking EC(nM)	Invasion Inhibition	
				100nM	10nM
1	10a		10	100%	55%
2	10b		100	62%	41%
3	10c		100	64%	58%
4	10d		1	78%	90%
5	10e		1	80%	53%
6	10f		10	100%	82%
7	10g		1	100%	100%
8	10h		100	73%	61%
9	10i		10	78%	41%
10	10j		1	82%	57%

^aIn this paper, EC (effective concentration) is defined as the concentration at which the compound blocks > 50% of **4** binding to CXCR4.

of compounds **1**, **5**, **21c**, **26** on U87CD4CCR5 cells, all showing no significant effect on blocking CCL5 stimulating CCR5. The compounds were unable to counteract the effect of CCL5 on CCR3 as well (data not shown).

Carrageenan-Induced Paw Edema Model. Carrageenan-induced mouse paw edema is a widely used test to assess anti-inflammatory activity in vivo. It is well-known that CXCR4 plays a key role in the recruitment of inflammatory cells to sites of inflammation. An apparent edema response was seen 24 h after the λ -carrageenan injection (compared to the contralateral paw that was injected with saline). On the basis of the rank order of in vitro assay results, 10 of the best compounds were investigated. Figure 3 shows the inflammation inhibition percentage by compound. Substances **10g**, **10e**, and **26** have more than 50% inhibitory effect on inflammation, which is superior to **5** and comparable to **4**, while the rest of the compounds revealed variable inhibition effects ranging from 20% to 50%. These data confirm that selected anti-CXCR4 drugs can inhibit inflammation as anticipated.

In Vivo Tumor Angiogenesis Assay (Matrigel Plugs). To determine the effect of the CXCR4/CXCL12 interaction on angiogenesis in vivo, an assay using Matrigel plugs to measure antiangiogenic activity of related compounds was

performed in nude mice as previously reported.¹⁶ A mixture of 2×10^5 MDA-MB-231 cells in 0.5 mL of growth factor-reduced Matrigel was implanted at two subcutaneous sites with the selected compound mixed in at 1 μ M. The rationale for initial mixing of the compounds into the Matrigel is that there is no route for the compounds to reach the cells within the Matrigel. From the following day, mice were treated with 10 mg/kg daily subcutaneous injections of selected compounds between the two plugs on the back of the mice. Ten days after the Matrigel implant, the mice were sacrificed and the Matrigel plugs were excised, photographed, weighed, and processed to measure hemoglobin content by using Drabkin's solution.¹⁷ When MDA-MB-231 cells successfully promote neovasculture formation within the Matrigel plug, these neovasculatures allow tumor cells to proliferate much better than those without neovasculatures.¹⁶ Therefore, the control group with better angiogenesis in the Matrigel plug showed more tumor cells than the treated group (Figure 4). The column graph in Figure 4 summarizes the percentage of antiangiogenic efficacy based on hemoglobin content in 10 Matrigel plugs per compound. All the selected compounds show a reasonable antiangiogenic effect with > 30% inhibition. Compound **26** furnishes the best inhibition efficacy of about 70%, which is comparable to the peptidic CXCR4

Table 3. Effects of Bis-pyrimidines as Blockers of CXCR4 Binding and Matrigel Invasion^a

Entry	Compd	R	R'	TN-binding	Invasion Inhibition	
				Blocking		
				EC (nM)	100nM	10nM
1	21a			1	93%	73%
2	21b			1	92%	62%
3	21c			1	95%	34%
4	17a			1	81%	65%
5	18a			10	65%	24%
6	18b			1	100%	77%
7	26			1	100%	84%

^a In this paper, EC (effective concentration) is defined as the concentration at which the compound blocks > 50% of **4** binding to CXCR4.

antagonist **4**. This result is consistent with all the in vitro and in vivo test results for compound **26**, which exhibits the best anti-CXCR4 activities in the full panel of in vitro assays.

Bleomycin Induced Lung Fibrosis Model. The bleomycin induced pulmonary fibrosis model in rodents has been widely used for evaluation of potential therapies. Treatment by **4** in mice with bleomycin-induced lung injury has been reported to significantly attenuate lung fibrosis.¹⁸ We used the same method to evaluate the therapeutic effect of compound **26** on bleomycin induced lung fibrosis because this compound is the most promising compound in all previous assays and in comparison to **4**. Lungs harvested 20 days after bleomycin treatment were analyzed histologically by H&E staining. Figure 5 shows representative photomicrographs of H&E stained sections. As reported in the literature, bleomycin caused marked alterations in lung architecture with increased interstitial wall thickness and mononuclear cell infiltrates.¹⁹ Mice receiving bleomycin and treated separately with **4** and compound **26** resulted in a decrease in interstitial and alveolar structural distortion (Figure 5B,C) compared to the lung tissue of untreated mice (Figure 5A). Compound **26** blocked lung fibrosis by 55% compared to **4** at 85% inhibition.

Uveal Melanoma Micrometastasis Mouse Model. Blocking CXCR4 has been shown to block metastasis of various cancers. Here, we tested its antimetastatic efficacy in a uveal melanoma micrometastasis nude mouse model.²⁰ Melanoma OMM2.3 cells overexpressing HGF/TGF- β /CXCR4/MMP2 were inoculated into the posterior chamber of the right eye. After 3 days, the treatment was started (and continued until sacrifice), and after one week, the eyes that developed tumors were enucleated. After 4 weeks, the mice were sacrificed and

hepatic tissues were collected, fixed in 10% formalin and paraffin-embedded. The samples were then sectioned and H&E stained (Figure 6). Six sections through the center of the liver were microscopically examined for the presence of micrometastases (< 100 μ m diameter), and the average number of micrometastases per section was determined. This has been shown to be a reliable and reproducible method for detecting hepatic micrometastases in this animal model.^{21,22} The micrometastases are very small cohorts of cells (a few to several), and the frequency of the micrometastatic colonies is not high. Because of the small size of the micrometastatic colonies, images were taken at 40 \times magnification (Figure 6). With the high magnification images, we could not find any field of view that shows a clear difference between treated and untreated livers (it is uncommon to find more than one colony per field of view). The column graph in Figure 6 shows the average number of the hepatic micrometastases throughout the liver counted under the microscope. The number of mice per group was 10. The total number of hepatic micrometastases in the treatment group, which was administered compound **26** or **4** at day-4 after uveal melanoma inoculation, was around 40. This was significantly less than the control group at around 90 ($p < 0.01$). Compound **26** decreased hepatic micrometastases by about 50% in a mouse model carrying human uveal melanoma with an efficacy similar to **4**.

Conclusions

We and others have shown that the CXCR4 antagonist T140 analogues, including **4**, bind to the CXCL12 binding site on CXCR4, block the CXCR4/CXCL12 interaction,^{11,23} and

intervene in the progression of cancer metastasis.^{11,24–26} Encouraged by these promising results observed with peptidic

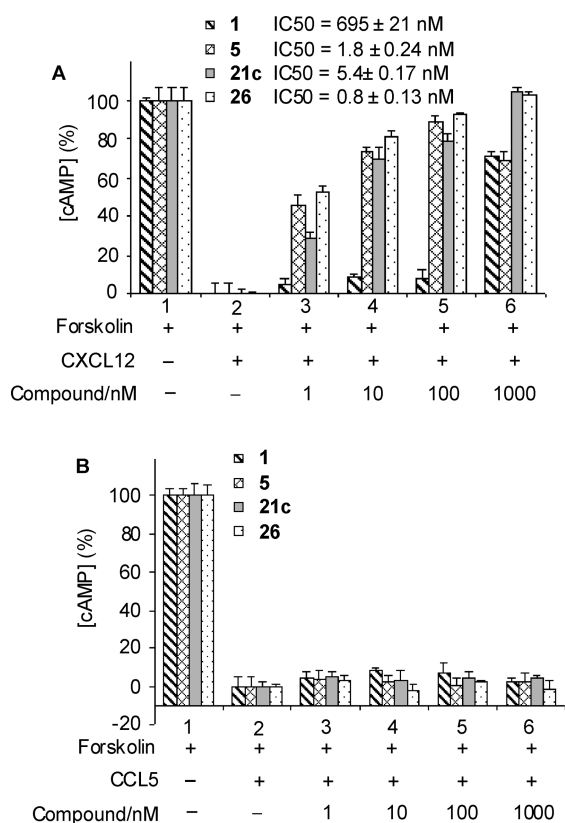


Figure 2. Comparison of inhibition of CXCR4/CXCL12-mediated cAMP modulation by anti-CXCR4 compounds. (A) CXCR4 positive cell line U87CD4CXCR4 was treated with chemokine CXCL12. (B) CCR5 positive cell line U87CD4CCR5 was treated with CCL5. With pretreatment (15 min at room temperature) of compounds, **1**, **5**, **21c**, or **26** at various concentrations, the effect of 150 ng/mL of CXCL12 or CCL5 on cAMP reduction in the presence of 5 μ M forskolin was measured by using the TR-FRET based LANCE assay kit. While our anti-CXCR4 compounds are effective in counteracting CXCL12 function at as low as 10 nM, **1** requires almost 1000 nM to significantly block CXCL12 function, which is 1000 times less efficient than our compounds in blocking the G α_i pathway. Compound **5** is our previously reported analogue; compounds **21c** and **26** are comparable or better than compound **5** in blocking CXCL12 function. The tested compounds have no effect on CCR5 cells.

agents, we sought to identify a novel series of potent, small-molecule antagonists that might prove to be practical and safe as antimetastatic agents. Currently, the metal-chelating cyclams and bicyclams represent the most studied class of nonpeptide CXCR4 inhibitors.¹² One of these, **1** has advanced as far as phase II clinical evaluation as an HIV entry inhibitor.^{13,14,27,28} However, it was withdrawn from that indication in response to adverse effects including cardiotoxicity.⁸ Currently, **1** has been FDA-approved for stem cell mobilization that requires only one-time administration. We have developed a series of small molecule CXCR4 antagonists that are devoid of metal chelating properties in an effort to develop a safer drug for long-term therapy. The present study reveals that *N,N'*-(1,4-phenylenebis(methylene))dipyrimidin-2-amines show potent CXCR4 antagonism and efficiency in a number of relevant in vitro and in vivo studies. Significantly, these compounds inhibit CXCL12-mediated chemotaxis and a series of pathway signaling events including cAMP action and angiogenesis. The results suggest that this class of compounds potentially inhibits the signaling cascade induced by CXCR4/CXCL12 and the associated invasion and homing capabilities.

Most chemokine receptors are shown to signal through the G α_i pathway, which results in an inhibition of adenylyl cyclase and a corresponding decrease in cAMP in the cells.²⁹ Another pathway that is believed to be activated is the G α_q pathway, which causes an increase in cytosolic Ca²⁺ levels. In the last two decades, many reports have demonstrated that the calcium flux assay cannot measure all G-protein coupled receptor function.³⁰ However, industrial and pharmaceutical companies still utilize the calcium flux assay as a gold standard to measure chemokine receptor function. Our CXCR4 compounds **26** and **21a** are effective in interrupting CXCL12/CXCR4-mediated cAMP modulation. However, they do not block Ca²⁺ flux induced by CXCR4/CXCL12 interaction through G α_q pathway (data not shown). Furthermore, our anti-CXCR4 compounds do not block ¹²⁵I-CXCL12 from binding to CXCR4, but CXCL12 can block these same compounds from binding to CXCR4.³¹ This may be due to the fact that CXCL12, a 9 kDa peptide, has multiple interaction sites on CXCR4,³² whereas our small CXCR4 compounds only block a single site related to homing and chemotaxis. Therefore, CXCL12 is still able to bind to CXCR4 when small-molecular-weight CXCR4 compounds are preincubated with cells before adding CXCL12. Intriguingly, the present class of anti-CXCR4 compounds can intervene in the G α_i signaling pathway (cAMP modulation) but not the G α_q pathway (Ca²⁺ flux).

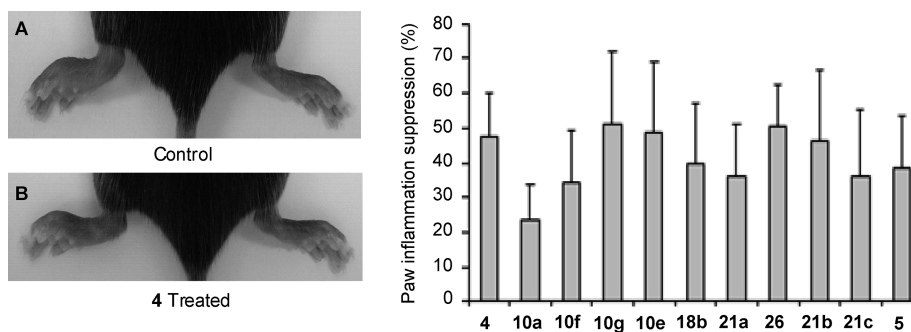


Figure 3. Suppression effect of anti-CXCR4 compounds on carrageenan-induced mouse paw inflammation. Acute paw inflammation was induced by subcutaneous injection of 50 μ L of λ -carrageenan in one hind paw. The mice in the treatment group were all administered CXCR4 antagonists at 10 mg/kg ip, while **4** was administered at 300 μ g/kg and 30 min following carrageenan challenge and daily thereafter. Control animals received corresponding ip injections of vehicle. (A) Control mouse with left paw induced inflammation by carrageenan. (B) **4** treated mouse with left paw induced inflammation by carrageenan with about 50% suppression. The bar graph shows that all tested compounds are effective at suppressing paw inflammation at different degrees. Compounds **10g**, **10e**, **26**, and **21b** showed effects comparable to **4**.

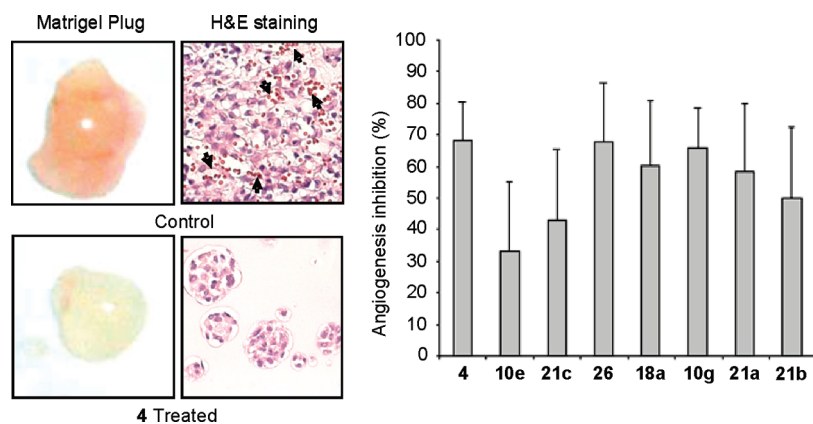


Figure 4. Inhibitory effect of anti-CXCR4 compounds on Matrigel plug angiogenesis assay in vivo. The mice in the CXCR4 antagonist-treated group received daily subcutaneous injections of the selected compounds (two plugs per mouse) at 10 mg/kg and **4** at 300 μ g/kg. Ten days after matrigel injection, the animals were sacrificed and the Matrigel plugs were excised, photographed, and sliced for H&E staining and processed for hemoglobin assay. Analogue **4**-treated Matrigel plugs revealed no significant angiogenesis, while the control group exhibited significantly more blood vessels clearly shown by H&E staining (the black arrows in the picture). The column graph shows the tested compounds can inhibit angiogenesis from 30% to 68%, while compound **26** delivers almost the same efficacy as **4** at about 70% angiogenesis inhibition.

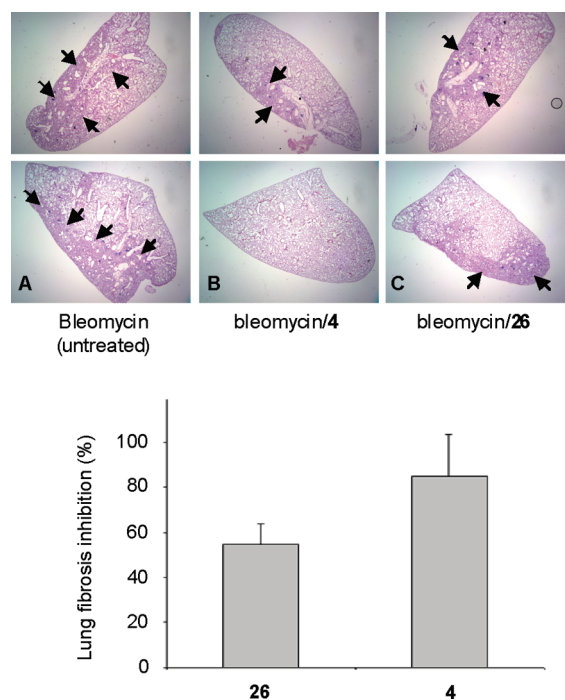


Figure 5. Inhibition effect of compound **26** compared to **4** on lung fibrosis induced by bleomycin. Representative H&E stained histopathologic sections of untreated (A), **4** was administered at 300 μ g/kg, ip (B), and **26** administered at 10 mg/kg, ip (C) lung tissues on day 20 after bleomycin treatment. Lung fibrosis is shown by small black arrows in the images. Column graph shows **4**- and **26**-treated groups experience a significant decrease in lung fibrosis.

These findings may present an opportunity for developing a safe drug that partially interrupts CXCL12/CXCR4, especially because the interplay between CXCL12 and CXCR4 is critical to normal physiology. For example, CXCR4 modulates contractility in adult cardiac myocytes by mediating Ca^{2+} flux.³³ Therefore, anti-CXCR4 compounds that do not interrupt Ca^{2+} flux may well be safer than **1**, which exhibits myocardial toxicity in addition to metal-chelating properties. In addition, the CXCR4/CXCL12 interaction is involved in the homing and retention of hematopoietic progenitor cells in the bone marrow, while CXCL12 also acts as a major

chemoattractant for stem cells and some differentiated cells in the pathological contexts of inflammation and tissue regeneration or repair.^{34–37} Therefore, the partial CXCR4 inhibitors reported here, which block chemotaxis and homing of the CXCR4-positive cells to the distant organ sites enriched with CXCL12 in their stroma, may present an alternative, safe option as chemopreventive drugs for cancer metastasis and tumor angiogenesis. Furthermore, we have demonstrated that **26** suppresses paw inflammation by 56%, inhibits angiogenesis by 70%, arrests lung fibrosis by 55%, and blocks uveal melanoma OMM2.3 (HGF/TGF- β /CXCR4/MMP2) micro-metastases by 50%, despite the fact that compound **26** has a fast blood clearance in mice ($t_{1/2} \sim 15$ min with intravenous injection). These data further support the role of CXCR4 in chemotaxis, motility, and invasion and reinforce its value as a target for therapeutic intervention in disease states where these phenomena play key roles such as cancer metastasis and inflammation.

Although the compound database represented by Tables 1–3 is sparse and the activity range is narrow, an intriguing SAR element is evident. It arises by classifying the blockade of **4** binding into two categories: high (1–10 nM) and low (100 nM). In this context, when one or both of the terminal aromatic rings are nitrogen deficient (i.e., either benzenoid or pyridinoid), then *ortho* substitution by a ring nitrogen, fluorine, or *N*-alkyl can lead to less effective competition with **4**. On the other hand, when both terminal rings are dipyrimidines, activity is high and substitution effects are marginal for the latter as shown, among others, by lead **26** (Table 3). Of course, the ring substitution pattern is decisive for phenomena associated with membrane passage and bio-distribution. The improved antagonistic effects of double pyrimidine substitution cannot be rationalized on a molecular level because the geometry of the specific binding site is presently unknown. However, a model of the binding of **1** to CXCR4 suggests a possible role for the dipyrimidine structure.²³

In conclusion, a novel class of small molecules, *N,N'*-(1,4-phenylenebis(methylene)) dipyrimidin-2-amines, especially compound **26**, have been identified by rational design and analysis of emerging structural and pharmacologic data as putative inhibitors of CXCR4/CXCL12 functions. The compelling features of **26** include effectiveness for (i) potent

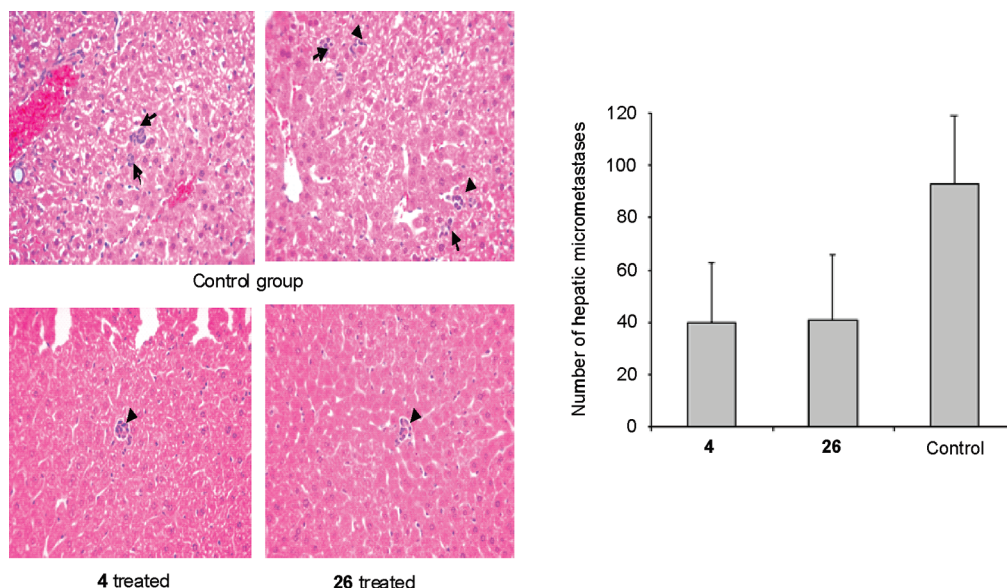


Figure 6. Inhibition effect of **26** compared to **4** in a uveal melanoma micrometastasis animal model. Hepatic tissues were collected and fixed in 10% formalin, processed, and H&E stained, and the number of hepatic micrometastasis was counted under a microscope. Micrometastatic clones are shown by small black arrows in the images. The murine model with ocular melanoma metastatic to the liver was treated with **4** at 300 $\mu\text{g}/\text{kg}$ ip or compound **26** at 10 mg/kg, ip once per day starting at fourth day after uveal melanoma inoculation. The animals presented significantly fewer micrometastases than those in the control (PBS-treated) group. Compound **26** decreased the numbers of hepatic micrometastases in a mouse model of human uveal melanoma with efficacy similar to **4**, both are about 50% inhibition.

inhibition of CXCR4/CXCL12 functions in vitro ($\text{IC}_{50} \sim 1$ nM), (ii) antiangiogenesis in vivo, (iii) suppression of inflammation in vivo, (iv) inhibition of lung fibrosis in vivo, and (v) blockade of uveal melanoma micrometastasis in vivo. In brief, compound **26** is an excellent anti-CXCR4 agent based on our in vitro and in vivo tests. However, the shortcomings of this compound are its fast blood clearance ($t_{1/2} \sim 15$ min with intravenous injection) and the lack of oral bioavailability. Thus, further improvement is needed to develop an orally available therapeutic drug. The physical properties of compound **26** make it suitable for nuclear imaging. Therefore, we are in a process of developing it as a positron emission tomography (PET) tracer to specifically image CXCR4-positive cells.

Experimental Section

Initial Screening of Anti-CXCR4 Small Molecules Based on a Binding Affinity Assay and Cell Invasion Assay. Binding affinity and cell invasion assays are basic assay tools that apply to the initial screening. MDA-MB-231 cells cultured in an 8-well slide chamber were preincubated with the testing compounds at 1, 10, 100, and 1000 nM. Then the cells were fixed with 4% formaldehyde and incubated with 50 nM biotinylated **4**, and followed by rhodamine staining. Matrigel invasion chambers from BD Bio-coat Cellware (San Jose, CA) were used for invasion assays. MDA-MB-231 cells were cultured on a layer of Matrigel in the upper chamber with testing compounds at 10 or 100 nM, while 200 ng/mL CXCL12 was added in the lower chamber as a chemoattractant. Detailed procedures for the binding and invasion assays have been described in previous publications.^{11,16,38}

cAMP Assay to Measure G α Function. Perkin-Elmer's LANCE cAMP assay kit (cat. no. AD0262), based on time-resolved fluorescence resonance energy transfer (TR-FRET), was used to determine whether our compounds could block cAMP modulation induced by the CXCR4/CXCL12 interaction. U87CD4CXCR4 cells (AIDS Consortium), U87CD4CCR3 cells (AIDS Consortium), or U87CD4CCR5 cells (AIDS Consortium) were used. The detailed procedures of the cAMP assay have been described in previous publications.⁹

Paw Inflammation Suppression Test. Acute inflammation was induced by subcutaneous injection of 50 μL of λ -carrageenan (1% w/v in saline) into one of the hind paws of female C57BL/6J mice (Jackson Laboratories); the other hind paw was used as a noninflammation control. In the treatment group, CXCR4 antagonists were administered ip at 10 mg/kg, while **4** was at 300 $\mu\text{g}/\text{kg}$, 30 min following carrageenan challenge and continued daily.^{18,39} The rationale for using 300 $\mu\text{g}/\text{kg}$ for compound **4** was that we found this concentration to be the minimum concentration to achieve the maximum efficacy of this compound in a breast cancer metastasis animal model.¹¹ All CXCR4 antagonists were dissolved in 10% DMSO and 90% of 45% (2-hydroxypropyl)- β -cyclodextrin (CD) in PBS. Control animals received corresponding ip injections of vehicle. The animals were sacrificed 74 h after induction of inflammation and 2 h after the last injection of CXCR4 antagonists. The final paws were photographed and measured for thickness from the "palm" to the back of the paw by a caliper. These were compared to the volume of carrageenan untreated contralateral paw to obtain the edema volume; the volume of the contralateral paw was subtracted from the volume of the carrageenan injected paw to obtain the edema volume. The inflammation suppression percentage was calculated by comparing the drug treated group to the control group.

In Vivo Angiogenesis Assay (Matrigel Plug). MDA-MB-231 cells (2×10^5) were mixed with the compound in 0.5 mL of growth factor-reduced matrigel (BD Biosciences, San Jose, CA) at 1 μM concentration and implanted subcutaneously into the flanks of nude mice (two plugs per mouse, six mice per group). The mice in the CXCR4 antagonist-treated group received daily subcutaneous injections of the selected drugs in the middle of the two plugs (two plugs per mouse) at 10 mg/kg, while **4** was administered at 300 $\mu\text{g}/\text{kg}$. Ten days after matrigel injection, the animals were sacrificed and the Matrigel plugs were excised. The excised plugs were photographed and processed for hemoglobin assay. The samples were homogenized in 100 μL of deionized water and cleared by centrifugation at 10000 rpm for 10 min. Then 20 μL of the supernatant was mixed with 100 μL of Drabkin's solution (Sigma, St. Louis, MO) to measure hemoglobin content. The mix was incubated at 52 $^\circ\text{C}$ for 10 min and

continuously at room temperature for 20 min. The absorbance was read at 540 nm in an ELISA plate reader.

Bleomycin Induced Lung Fibrosis Mouse Model. Mice were anesthetized by isoflurane inhalation; the trachea was exposed using sterile techniques and 4 U/kg bleomycin (Sigma) in 100 μ L of PBS or PBS vehicle was injected into the tracheal lumen. After inoculation, the incision was closed and the animals were allowed to recover. Each group has 10 mice that received 300 μ g/kg of **4**, 10 mg/kg of compound **26** or saline intraperitoneally 1 day before bleomycin treatment and daily for 20 days. All mice tolerated the antagonist well. Lungs harvested 20 days after bleomycin treatment were analyzed histologically by H&E staining and imaged under microscope.

Uveal Melanoma Micrometastasis Mouse Model. The female nude mice were divided into three groups: two treatment groups and one control group, with 10 mice in each group. On day 0, each mouse was inoculated with 1×10^6 OMM2.3 cells expressing HGF/TGF- β /CXCR4/MMP2 into the posterior chamber of right eye. On day 3, mice were treated with 10 mg/kg compound **26** or 300 μ g/kg **4** in 0.1 mL volume of 45% CD daily by ip injection, whereas the control mice were ip injected with 0.1 mL 45% CD only. On day 7, eyes with tumors were enucleated. The growth of tumor was checked by histological methods. On day 28, hepatic tissues were collected and fixed in 10% formalin, processed, H&E stained, and the number of hepatic micrometastases was counted under microscope. Six sections through the center of the liver were microscopically examined (Olympus BX41, Tokyo, Japan) for the presence of micrometastases (< 100 μ m diameter) and the average number of micrometastases per section was determined.

Chemistry: General. Proton and carbon NMR spectra were recorded on INOVA-400 (400 MHz) or INOVA-600 (600 MHz) spectrometers. The spectra obtained in deuteriochloroform (CDCl_3) or dimethyl sulfoxide- d_6 ($\text{DMSO-}d_6$) were referenced to the residual solvent peak. Mass spectra were recorded on a JEOL spectrometer at Emory University Mass Spectrometry Center. Elemental analyses were performed by Atlantic Microlab, Inc. Norcross, GA. Flash column chromatography was carried out with Scientific Absorbent Incorporated Silica Gel 60. Analytical thin layer chromatography (TLC) was performed on precoated glass backed plates from Scientific Adsorbents Incorporated (Silica Gel 60 F₂₅₄; 0.25 mm thickness). Plates were visualized using ultraviolet, iodine vapors, or phosphomolybdic acid (PMA). Preparation of compounds **3**, **5**, and **6** has been documented in our previous report.⁹ All final compounds were > 98% pure, which was confirmed by a Beckman HPLC system using Nova Pak C18 4 μ m 3.9 mm \times 150 mm column (Waters) and methanol/water (65:35) with 0.1% triethylamine as an eluent. Elemental analyses were performed by Atlantic Microlab, Inc. Norcross, GA and were within $\pm 0.4\%$ of the theoretical values.

***N,N'*-(1,4-Phenylenebis(methylene))bis(6-fluoropyridin-2-amine) (8a).** A mixture of terephthalaldicarboxaldehyde (268 mg, 2.0 mmol) and 6-fluoro-2-aminopyridin (0.47 g, 4.2 mmol) in 1, 2-dichloroethane (20 mL) was treated with triacetoxyborohydride (1.27 g, 6.0 mmol) and HOAc (0.24 mL, 4.0 mmol). After stirring at room temperature under an argon atmosphere until the disappearance of the starting materials, the reaction was quenched by adding aqueous NaOH (10 mL, 1.0 N). The resulting mixture was extracted with ethyl acetate (3 \times 15 mL), and the combined organic layers were washed with brine, dried over anhydrous MgSO_4 , and concentrated in vacuo. Purification by flash column chromatography (silica gel, hexane/ethyl acetate, 3/1 with 0.5% NH_4OH) gave the title compound **8a** (0.42 g, 64%) as a white solid: mp 182–185 $^\circ\text{C}$ (dec). ^1H NMR (400 MHz, $\text{DMSO-}d_6$) δ 7.48 (dd, $J = 16.8, 7.9$ Hz, 2H), 7.43 (t, $J = 6.0, 6.0$ Hz, 2H), 7.26 (s, 4H), 6.35 (dd, $J = 8.1, 2.4$ Hz, 2H), 6.08 (dd, $J = 7.6, 2.2$ Hz, 2H), 4.37 (d, $J = 6.0$ Hz, 4H). ^{13}C NMR (100 MHz, $\text{DMSO-}d_6$) δ 162.79, 158.23, 141.43, 138.30, 127.26, 104.49,

93.56, 43.96. HRMS calcd for $\text{C}_{18}\text{H}_{17}\text{F}_2\text{N}_4$ 327.14213 $[\text{M} + \text{H}]^+$, found 327.14156. Anal. ($\text{C}_{18}\text{H}_{16}\text{F}_2\text{N}_4$) C, H, N.

***N,N'*-(1,4-Phenylenebis(methylene))bis(5-fluoropyridin-2-amine) (8b).** Starting with terephthalaldicarboxaldehyde (0.27 g, 2.0 mmol) and 5-fluoropyridin-2-amine (0.45 g, 4.0 mmol) by treating with triacetoxyborohydride (1.27 g, 6.0 mmol), the same procedure to compound **8a** furnished the title product **8b** (0.40 g, 61%) as a white solid: mp 163–165 $^\circ\text{C}$ (dec). ^1H NMR (600 MHz, CDCl_3) δ 7.90 (d, $J = 3.0$ Hz, 2H), 7.33 (dt, $J = 8.8, 8.8, 3.1$ Hz, 2H), 7.24 (s, 4H), 7.01 (t, $J = 5.9, 5.9$ Hz, 2H), 6.51 (dd, $J = 9.2, 3.6$ Hz, 2H), 4.38 (d, $J = 6.0$ Hz, 4H). ^{13}C NMR (150 MHz, CDCl_3) δ 155.69, 152.47, 138.70, 133.42, 125.03, 108.78, 44.40; HRMS calcd for $\text{C}_{18}\text{H}_{17}\text{F}_2\text{N}_4$ 327.14213 $[\text{M} + \text{H}]^+$, found 327.14117. Anal. ($\text{C}_{18}\text{H}_{16}\text{F}_2\text{N}_4$) C, H, N.

4-((Pyrimidin-2-ylamino)methyl)benzaldehyde (9). In a 500 mL one-necked round-bottomed flask equipped with a stirrer, terephthalaldicarboxaldehyde (5.36 g, 40 mmol), 2-amino-pyrimidine (3.91 g, 41 mmol), and acetic acid (4.7 mL, 80 mmol) were mixed in 1,2-dichloroethane (250 mL). After being stirred at room temperature until 2-amino-pyrimidine completely dissolved (approximately 10 min), 4 Å molecular sieves (20 g) were added to the mixture. After being stirred for 10 min, the resulting mixture was treated with sodium triacetoxyborohydride (25.43 g, 120 mmol). After being stirred for 24 h at room temperature under an argon atmosphere, the reaction was quenched by adding aqueous NaOH (150 mL, 1.0 N). The resulting mixture was extracted with ethyl acetate (3 \times 200 mL), and the combined organic layers were washed with brine, dried over anhydrous MgSO_4 , and concentrated in vacuo to give the alcohol intermediate **S1**, which was purified by column chromatography (ethyl acetate) to give alcohol **S1** as a white solid (7.32 g, 86%): mp 120–121 $^\circ\text{C}$ (dec). ^1H NMR (400 MHz, CDCl_3) δ 8.30 (d, $J = 4.8$ Hz, 2H), 7.35 (s, 4H), 6.57 (t, $J = 4.8$ Hz, 1H), 5.42 (bs, 1H), 4.69 (d, $J = 5.6$ Hz, 2H), 4.64 (d, $J = 5.6$ Hz, 2H), 1.83 (t, $J = 5.6$ Hz, 1H). ^{13}C NMR (100 MHz, CDCl_3) δ 162.27, 157.93, 140.71, 138.75, 126.74, 126.36, 110.14, 62.73, 43.65. HRMS calcd for $\text{C}_{12}\text{H}_{14}\text{N}_3\text{O}$ 216.11369 $[\text{M} + \text{H}]^+$, found 216.11284. To a solution of the alcohol **S1** (2.22 g, 10.3 mmol) in CH_2Cl_2 (50 mL) was added Dess–Martin periodinane (5.24 g, 12.3 mmol) at 0 $^\circ\text{C}$. After being stirred for 10 min, the reaction mixture was allowed to warm to room temperature and was stirred for another 1 h. The reaction mixture was diluted with diethyl ether (100 mL) and quenched by saturated aqueous NaHCO_3 (50 mL) and Na_2SO_3 (50 mL). The organic phase was separated, and the aqueous phase was further extracted with diethyl ether (3 \times 20 mL). The combined organics were dried over MgSO_4 , filtered, and concentrated under reduced pressure. The residue was purified through flash column chromatography (ethyl acetate) to furnish aldehyde **9** (2.07 g, 94%) as a white solid: mp 114–115 $^\circ\text{C}$ (dec). ^1H NMR (400 MHz, CDCl_3) δ 10.00 (s, 1H), 8.29 (d, $J = 4.8$ Hz, 2H), 7.85 (d, $J = 8.2$ Hz, 2H), 7.52 (d, $J = 8.1$ Hz, 2H), 6.60 (t, $J = 4.8, 4.8$ Hz, 1H), 5.82 (bs, 1H), 4.75 (d, $J = 6.3$ Hz, 2H). ^{13}C NMR (100 MHz, CDCl_3) δ 192.13, 162.30, 158.35, 146.69, 135.69, 130.31, 127.86, 111.52, 45.25. HRMS calcd for $\text{C}_{12}\text{H}_{12}\text{N}_3\text{O}$ 214.09804 $[\text{M} + \text{H}]^+$, found 214.09718.

***N*-(4-((Phenylamino)methyl)pyrimidin-2-amine) (10a)**
General Procedure A. A mixture of aldehyde **9** (0.32 g, 1.5 mmol) and aniline (0.15 g, 1.6 mmol) in 1,2-dichloroethane (15 mL) was treated with sodium triacetoxyborohydride (0.48 mg, 2.25 mmol). After being stirred at room temperature overnight, the reaction mixture was quenched by adding aqueous NaOH (10 mL, 1.0 N) and extracted with ethylacetate (2 \times 30 mL). The combined organic phases were washed by brine, dried over anhydrous MgSO_4 , and filtered and concentrated under reduced pressure. The residue was purified by column chromatography (hexanes/ethyl acetate, 1/1) to afford product **10a** (0.41 mg, 94%) as a white solid: mp 131–132 $^\circ\text{C}$ (dec). ^1H NMR (400 MHz, CDCl_3) δ 8.27 (d, $J = 4.7$ Hz, 2H), 7.34 (s, 4H), 7.21–7.15 (m, 2H), 6.72 (tt, $J = 7.4, 7.4, 1.0, 1.0$ Hz, 1H), 6.65–6.0 (m, 2H), 6.54 (t, $J = 4.8, 4.8$ Hz, 1H), 5.59 (s, 1H), 4.63 (d, $J = 5.9$ Hz, 2H), 4.32 (s, 2H), 4.04 (s, 1H).

^{13}C NMR (100 MHz, CDCl_3) δ 162.48, 160.40, 158.33, 148.27, 138.66, 138.29, 129.47, 127.96, 117.77, 113.02, 111.12, 48.19, 45.31. HRMS calcd for $\text{C}_{18}\text{H}_{19}\text{N}_4$ 291.16097, $[\text{M} + \text{H}]^+$ found 291.1033. Anal. ($\text{C}_{18}\text{H}_{18}\text{N}_4$) C, H, N.

***N*-(4-((2-Fluorophenylamino)methyl)benzyl)pyrimidin-2-amine (10b)**. Starting from aldehyde **9** (53.4 mg, 0.25 mmol) and 2-fluoroaniline (29.2 mg, 0.26 mmol), general procedure A gave **10b** (44.2 mg, 57%) as a white solid: mp 126–128 °C (dec). ^1H NMR (400 MHz, CDCl_3) δ 8.30 (d, $J = 4.8$ Hz, 2H), 7.35 (s, 4H), 7.01–6.94 (m, 2H), 6.69–6.61 (m, 2H), 6.57 (t, $J = 4.8$, 4.8 Hz, 1H), 5.52 (bs, 1H), 4.65 (d, $J = 6.0$ Hz, 2H), 4.36 (s, 2H), 4.32 (bs, 1H). ^{13}C NMR (100 MHz, CDCl_3) δ 162.47, 158.26, 151.68 (d, $J = 237.5$ Hz), 138.58 (d, $J = 32.6$ Hz), 136.75, 136.64, 128.02, 127.81, 124.76, 116.98, 114.55, 112.44, 110.98, 47.70, 45.29. HRMS calcd for $\text{C}_{18}\text{H}_{18}\text{FN}_4$ 309.15155 $[\text{M} + \text{H}]^+$, found 309.15050. Anal. ($\text{C}_{18}\text{H}_{17}\text{FN}_4$) C, H, N.

***N*-(4-((Pyridin-2-ylamino)methyl)benzyl)pyrimidin-2-amine (10c)**. Starting from aldehyde **9** (0.43 g, 2.0 mmol) and 2-aminopyridine (0.23 g, 2.4 mmol) by treatment with sodium triacetoxymethylborohydride (0.64 g, 3.0 mmol) and HOAc (0.13 mL, 2.2 mmol), general procedure A gave white solid, which was washed by methanol to afford **10c** (0.35 g, 61%) as a white solid: mp 172–174 °C (dec). ^1H NMR (400 MHz, CDCl_3) δ 8.30 (d, $J = 4.8$ Hz, 2H), 8.11 (d, $J = 4.8$ Hz, 1H), 7.43–7.39 (m, 1H), 7.34 (s, 4H), 6.62–6.58 (m, 1H), 6.57 (t, $J = 4.8$, 4.8 Hz, 1H), 6.37 (d, $J = 8.4$ Hz, 1H), 5.41 (bs, 1H), 4.88 (bs, 1H), 4.64 (d, $J = 6.0$ Hz, 2H), 4.50 (d, $J = 6.0$ Hz, 2H). ^{13}C NMR (150 MHz, CDCl_3) δ 162.48, 158.65, 158.33, 148.05, 138.36, 138.29, 137.90, 127.96, 127.86, 113.37, 111.14, 107.11, 46.24, 45.30. HRMS calcd for $\text{C}_{17}\text{H}_{18}\text{N}_5$ 292.15622 $[\text{M} + \text{H}]^+$, found 292.15518. Anal. ($\text{C}_{17}\text{H}_{17}\text{N}_5$) C, H, N.

***N*-(4-((5-Fluoropyridin-2-ylamino)methyl)benzyl)pyrimidin-2-amine (10d)**. Starting from aldehyde **9** (0.22 mg, 1.0 mmol) and 5-fluoro-2-aminopyridine (0.12 g, 1.0 mmol) by treatment with sodium triacetoxymethylborohydride (0.32 g, 1.5 mmol) and HOAc (0.06 mL, 1.0 mmol), general procedure A gave **10d** (0.28 mg, 90%) as a white solid: mp 167–169 °C (dec). ^1H NMR (400 MHz, CDCl_3) δ 8.29 (d, $J = 4.8$ Hz, 2H), 7.96 (d, $J = 2.8$ Hz, 1H), 7.33 (s, 4H), 7.21–7.16 (m, 1H), 6.57 (t, $J = 4.8$, 4.8 Hz, 1H), 6.32 (dd, $J = 9.2$, 3.2 Hz, 1H), 5.49 (bs, 1H), 4.85 (bs, 1H), 4.63 (d, $J = 6.0$ Hz, 2H), 4.46 (d, $J = 6.0$ Hz, 2H). ^{13}C NMR (150 MHz, CDCl_3) δ 162.43, 158.35, 155.44, 153.72, 138.38, 138.26, 134.80, 127.96, 127.88, 125.61, 111.19, 107.40, 46.73, 45.30. HRMS calcd for $\text{C}_{17}\text{H}_{17}\text{FN}_5$ 310.14680 $[\text{M} + \text{H}]^+$, found 310.14588. Anal. ($\text{C}_{17}\text{H}_{16}\text{FN}_5$) C, H, N.

***N*-(4-((6-Fluoropyridin-2-ylamino)methyl)benzyl)pyrimidin-2-amine (10e)**. Starting from aldehyde **9** (0.43 g, 2.0 mmol) and 6-fluoro-2-aminopyridine (0.25 g, 2.4 mmol) by treatment with sodium triacetoxymethylborohydride (0.64 g, 3.0 mmol) and HOAc (0.12 mL, 2.2 mmol), general procedure A gave **10e** (0.46 g, 73%) as a white solid: mp 170–171 °C (dec). ^1H NMR (400 MHz, CDCl_3) δ 8.24 (d, $J = 4.4$ Hz, 2H), 7.66 (t, $J = 6.2$ Hz, 1H), 7.51–7.40 (m, 2H), 7.24 (s, 4H), 6.55 (t, $J = 4.8$ Hz, 1H), 6.34 (dd, $J = 8.0$, 2.4 Hz, 1H), 6.08 (dd, $J = 8.0$, 2.8 Hz, 1H), 4.45 (d, $J = 6.4$ Hz, 2H), 4.35 (d, $J = 6.0$ Hz, 2H). ^{13}C NMR (150 MHz, CDCl_3) δ 162.77, 162.26, 158.22, 157.96, 141.42, 138.88, 137.99, 127.14, 126.99, 110.17, 104.46, 93.52, 43.96, 43.62. HRMS calcd for $\text{C}_{17}\text{H}_{18}\text{FN}_5$ 310.14680 $[\text{M} + \text{H}]^+$, found 310.14954. Anal. ($\text{C}_{17}\text{H}_{16}\text{FN}_5$) C, H, N.

***N*-(4-((5-Chloropyridin-2-ylamino)methyl)benzyl)pyrimidin-2-amine (10f)**. Starting from aldehyde **9** (0.22 g, 1.0 mmol) and 5-chloro-2-aminopyridine (0.14 g, 1.1 mmol) by treatment with sodium triacetoxymethylborohydride (0.32 g, 1.5 mmol) and HOAc (0.06 mL, 1.1 mmol), general procedure A gave **10f** (0.20 g, 60%) as a white solid: mp 163–165 °C (dec). ^1H NMR (400 MHz, $\text{DMSO}-d_6$) δ 8.24 (d, $J = 4.8$ Hz, 2H), 7.93 (d, $J = 2.8$ Hz, 1H), 7.66 (t, $J = 6.4$ Hz, 1H), 7.41 (dd, $J = 8.8$, 2.4 Hz, 1H), 7.25 (d, $J = 6.0$ Hz, 1H), 7.23 (s, 4H), 6.55 (t, $J = 4.8$, 4.8 Hz, 1H), 6.51 (d, $J = 8.8$ Hz, 1H), 4.44 (d, $J = 6.4$ Hz, 2H), 4.39 (d, $J = 6.4$ Hz, 2H). ^{13}C NMR (150 MHz,

$\text{DMSO}-d_6$) δ 162.27, 158.00, 157.26, 145.46, 138.81, 138.29, 136.48, 127.12, 126.97, 117.43, 110.18, 109.61, 44.08, 43.63. HRMS calcd for $\text{C}_{17}\text{H}_{17}\text{ClN}_5$ 326.11725 $[\text{M} + \text{H}]^+$, found 326.11638. Anal. ($\text{C}_{17}\text{H}_{16}\text{ClN}_5$) C, H, N.

***N*-(4-((6-Chloropyridin-2-ylamino)methyl)benzyl)pyrimidin-2-amine (10g)**. Starting from aldehyde **9** (0.21 g, 1.0 mmol) and 6-chloro-2-aminopyridine (0.14 g, 1.1 mmol) by treatment with sodium triacetoxymethylborohydride (0.32 g, 1.5 mmol) and HOAc (0.064 mL, 1.1 mmol), general procedure A gave **10g** (0.22 g, 67%) as a white solid: mp 148–150 °C (dec). ^1H NMR (400 MHz, $\text{DMSO}-d_6$) δ 8.24 (d, $J = 4.8$ Hz, 2H), 7.67 (t, $J = 6.0$ Hz, 1H), 7.43 (t, $J = 6.0$ Hz, 1H), 7.37 (t, $J = 7.6$ Hz, 1H), 7.25 (s, 4H), 6.55 (t, $J = 4.8$ Hz, 1H), 6.49 (d, $J = 7.2$ Hz, 1H), 6.42 (d, $J = 8.0$ Hz, 1H), 4.46 (d, $J = 6.4$ Hz, 2H), 4.37 (d, $J = 6.0$ Hz, 2H). ^{13}C NMR (100 MHz, $\text{DMSO}-d_6$) δ 162.26, 158.89, 157.97, 148.39, 139.59, 138.93, 137.89, 127.24, 126.99, 110.20, 110.17, 106.42, 43.99, 43.62. HRMS Calcd for $\text{C}_{17}\text{H}_{17}\text{ClN}_5$ 326.11725 $[\text{M} + \text{H}]^+$, found 326.11640. Anal. ($\text{C}_{17}\text{H}_{16}\text{ClN}_5$) C, H, N.

***N*-(4-((2-(Pyrrolidin-1-yl)phenylamino)methyl)benzyl)pyrimidin-2-amine (10h)**. A solution of boc-protected 2-(pyrrolidin-1-yl)aniline (0.26 g, 1.0 mmol) in CH_2Cl_2 (5 mL) was treated with HCl solution in dioxane (5 mL, 4 M in dioxane). After being stirred for 6 h at room temperature, the solvent was removed under reduced pressure to afford a yellow solid (0.27 g). The yellow solid prepared above was dissolved in 1,2-dichloroethane (20 mL), to which was added aldehyde **9** (0.20 g, 0.9 mmol) and HOAc (0.06 mL, 1.0 mmol). The resulting light-brown solution was treated with triacetoxymethylborohydride (0.32 mg, 1.5 mmol), and general procedure A gave the title product **10h** (0.31 g, 85%, 2 steps) as a pale-white solid: mp 124–126 °C (dec). ^1H NMR (400 MHz, CDCl_3) δ 8.27 (d, $J = 4.8$ Hz, 2H), 7.33–7.39 (m, 4H), 7.05 (dd, $J = 7.6$, 1.6 Hz, 1H), 6.95 (td, $J = 7.6$, 1.6 Hz, 1H), 6.70 (td, $J = 7.6$, 1.6 Hz, 1H), 6.59 (dd, $J = 7.6$, 1.6 Hz, 1H), 6.55 (t, $J = 4.8$ Hz, 1H), 5.68 (bs, 1H), 4.91 (bs, 1H), 4.65 (d, $J = 6.0$ Hz, 2H), 4.36 (d, $J = 5.2$ Hz, 2H), 3.04–3.07 (m, 4H), 1.88–1.95 (m, 4H). ^{13}C NMR (100 MHz, CDCl_3) δ 162.48, 158.22, 143.51, 139.23, 137.97, 137.42, 127.93, 127.69, 124.22, 118.56, 117.10, 110.86, 110.47, 51.42, 48.22, 45.34, 24.23. HRMS calcd for $\text{C}_{22}\text{H}_{26}\text{N}_5$ 360.21882 $[\text{M} + \text{H}]^+$, found 360.21805. Anal. ($\text{C}_{22}\text{H}_{25}\text{N}_5$) C, H, N.

***N*-(4-((3-(Pyrrolidin-1-yl)phenylamino)methyl)benzyl)pyrimidin-2-amine (10i)**. The boc-protected 3-(pyrrolidin-1-yl)aniline (0.29 mg, 1.1 mmol) was converted to **10i** (0.19 g, 58%, 2 steps) according to the procedure described above for **10h** as a pale-white solid: mp 136–138 °C (dec). ^1H NMR (400 MHz, CDCl_3) δ 8.19 (bs, 2H), 7.38–7.33 (m, 4H), 7.06 (t, $J = 8.0$ Hz, 1H), 6.50 (t, $J = 4.8$, 4.8 Hz, 1H), 6.28 (t, $J = 5.6$, 5.6 Hz, 1H), 6.03 (dd, $J = 6.0$, 2.0 Hz, 2H), 5.88 (t, $J = 2.0$, 2.0 Hz, 1H), 4.64 (d, $J = 5.6$, 5.6 Hz, 2H), 4.34 (s, 2H), 4.01 (bs, 1H), 3.30–3.24 (m, 4H), 2.01–1.95 (m, 4H). ^{13}C NMR (100 MHz, CDCl_3) δ 162.41, 158.14, 149.36, 149.15, 139.10, 138.04, 129.97, 127.90, 110.77, 102.24, 101.17, 96.34, 48.23, 47.65, 45.29, 25.54. HRMS calcd for $\text{C}_{22}\text{H}_{26}\text{N}_5$ 360.21882 $[\text{M} + \text{H}]^+$, found 360.21805. Anal. ($\text{C}_{22}\text{H}_{25}\text{N}_5$) C, H, N.

***N*-(4-((4-(Pyrrolidin-1-yl)phenylamino)methyl)benzyl)pyrimidin-2-amine (10j)**. The boc-protected 4-(pyrrolidin-1-yl)aniline (0.26 g, 1.0 mmol) was converted to **10j** (0.30 g, 92%, 2 steps) according to the procedure described above for **10h** as a pale-white solid: mp 149–153 °C (dec). ^1H NMR (400 MHz, CDCl_3) δ 8.30 (d, $J = 4.8$ Hz, 2H), 7.31–7.37 (m, 4H), 6.65 (bs, 2H), 6.57 (t, $J = 4.8$ Hz, 1H), 6.55 (bs, 2H), 5.41 (bs, 1H), 4.63 (d, $J = 5.6$ Hz, 2H), 4.27 (bs, 2H), 3.63 (bs, 1H), 3.20 (bs, 4H), 1.95–1.99 (m, 4H). ^{13}C NMR (100 MHz, CDCl_3) δ 162.48, 158.26, 142.07, 139.21, 138.00, 128.04, 127.87, 115.19, 113.31, 110.97, 49.63, 48.51, 25.44. HRMS calcd for $\text{C}_{22}\text{H}_{26}\text{N}_5$ 360.21882 $[\text{M} + \text{H}]^+$, found 360.21829. Anal. ($\text{C}_{22}\text{H}_{25}\text{N}_5$) C, H, N.

***N,N'*-(1,4-Phenylenebis(methylene))bis(5-fluoropyrimidin-2-amine) (13)**. A mixture of 2-chloro-5-fluoropyrimidine (0.92 g, 6.9 mmol), 1,4-phenylenedimethanamine (0.45 g, 3.3 mmol), and cesium carbonate (2.58 g, 7.9 mmol) in DMF (25 mL) was stirred at 100 °C overnight. After removing the solvent under reduced pressure, the yellow residue was washed with H_2O and

hot ethanol to give the title product **13** (0.65 g, 60%) as pale-yellow solid: mp 220–226 °C (dec). ¹H NMR (400 MHz, DMSO-*d*₆) δ 8.33 (s, 4H), 7.78 (t, *J* = 6.0 Hz, 2H), 7.21 (s, 4H), 4.41 (d, *J* = 6.0 Hz, 4H). ¹³C NMR (100 MHz, DMSO-*d*₆) δ 159.47, 151.60, 145.49, 138.44, 126.86, 44.24. HRMS calcd for C₁₆H₁₅F₂N₆ 329.13263 [M + H]⁺, found 329.13192. Anal. (C₁₆H₁₄F₂N₆) C, H, N.

***N,N'*-(1,4-Phenylenebis(methylene))bis(4,6-dichloro-1,3,5-triazin-2-amine) (15)**. To a solution of cyanuric chloride (1.94 g, 10.5 mmol) in THF (70 mL) was added 1,4-phenylenedimethanamine (0.681 g, 5.0 mmol) at 0 °C in portionwise, followed by an addition of NaHCO₃ (1.05 g, 12.5 mmol). After being stirred overnight at 0 °C, the reaction mixture was warmed to room temperature and stirred for additional 2 h. The solvent was removed under reduced pressure, and the white solid residue was sequentially washed with water and ethanol to afford pure title compound **15** (2.04 g, 94%) as a white solid: mp > 400 °C (dec). ¹H NMR (400 MHz, DMSO-*d*₆) δ 9.61 (t, *J* = 6.1, 6.1 Hz, 2H), 7.27 (s, 4H), 4.50 (d, *J* = 6.2 Hz, 4H). ¹³C NMR (150 MHz, DMSO-*d*₆) δ 169.51, 168.63, 165.46, 136.51, 127.45, 43.71. HRMS calcd for C₁₄H₁₁Cl₄N₈ 430.98608 [M + H]⁺, found 430.96623. Anal. (C₁₄H₁₀Cl₄N₈) C, H, N.

***N,N'*-(1,4-Phenylenebis(methylene))bis(2-fluoropyrimidin-4-amine) (17a)**. To a solution of 1,4-phenylenedimethanamine (1.36 g, 10 mmol) in DMF (50 mL) was added 2,4-difluoropyrimidine (2.56 g, 22 mmol) and *N,N*-diisopropylethylamine (6.10 mL, 35 mmol) at room temperature. The resulting mixture was heated to 60 °C and stirred until the starting material disappeared from TLC plate. The reaction mixture was cooled down to ambient temperature, poured into ice water (20 mL), and extracted with ethyl acetate (3 × 5 mL). The combined organic layers were washed with brine, dried over anhydrous MgSO₄, and concentrated in vacuo. The crude was purified by flash column chromatography (silica gel, MeOH/CH₂Cl₂, 0 → 25%) to give the title compound **17a** (2.49 g, 76%), as a white solid: mp 267–268 °C (dec). ¹H NMR (600 MHz, DMSO-*d*₆) δ 7.93 (d, *J* = 4.2 Hz, 2H), 7.28 (s, 4H), 6.38 (bs, 1H), 6.34 (bs, 1H), 6.47 (t, *J* = 4.8 Hz, 2H), 4.47 (d, *J* = 6 Hz, 4H). ¹³C NMR (150 MHz, DMSO-*d*₆) δ 165.22, 161.98, 156.20, 137.43, 127.60, 104.25, 43.17. HRMS calcd for C₁₆H₁₅F₂N₆ 329.13263 [M + H]⁺, found 329.13230. Anal. (C₁₆H₁₄F₂N₆) C, H, N.

***N,N'*-(1,4-Phenylenebis(methylene))bis(2,5-difluoropyrimidin-4-amine) (17b)**. Starting with 1,4-phenylenedimethanamine (1.36 g, 10 mmol) and 2,4,5-trifluoropyrimidine (2.95 g, 22 mmol), the same procedure to compound **17a** furnished the title product **17b** (2.77 g, 76%) as a white solid. ¹H NMR (600 MHz, DMSO-*d*₆) δ 8.06 (d, *J* = 3 Hz, 2H), 7.27 (s, 4H), 6.82 (bs, 2H), 4.52 (d, *J* = 6 Hz, 4H). ¹³C NMR (150 MHz, DMSO-*d*₆) δ 157.89, 156.52, 145.00, 143.38, 137.17, 127.39, 43.05. HRMS calcd for C₁₆H₁₃F₄N₆ 365.11378 [M + H]⁺, found 365.11325.

***N,N'*-(1,4-Phenylenebis(methylene))bis(2-methoxy-pyrimidin-4-amine) (18a)**. A solution of **17a** (1.31 g, 4 mmol) in methanol (20 mL) was treated with thionyl chloride (2.91 mL, 40 mmol) at room temperature. The resulting mixture was stirred, at which time all starting material was consumed. The solvent was removed under reduced pressure. The residue was dissolved in ethyl acetate (20 mL) and washed with aqueous NaOH (10 mL, 1N). The organic layer was separated, dried over anhydrous MgSO₄, and concentrated in vacuo. The crude was purified by flash column chromatography (silica gel, MeOH/CH₂Cl₂, 0 → 25%) to give the title compound **18a** (1.35 g, 96%) as a white solid: mp 187–188 °C (dec). ¹H NMR (600 MHz, DMSO-*d*₆) δ 7.89 (t, *J* = 6 Hz, 2H), 7.83 (bs, 2H), 7.26 (s, 4H), 6.16 (bs, 2H), 4.45 (bs, 4H), 3.74 (s, 6H). ¹³C NMR (150 MHz, DMSO-*d*₆) δ 165.06, 163.81, 155.29, 138.12, 127.46, 100.32, 53.53, 42.92. HRMS calcd for C₁₈H₂₁N₆O₂ 353.17260 [M + H]⁺, found 353.17221. Anal. (C₁₈H₂₀N₆O₂) C, H, N.

***N,N'*-(1,4-Phenylenebis(methylene))bis(5-fluoro-2-methoxy-pyrimidin-4-amine) (18b)**. Starting with compound **17b** (1.68 g, 4.6 mmol), the same procedure to compound **18a** furnished the title product **18b** (1.66 g, 93%) as a white solid: mp 158–160 °C

(dec). ¹H NMR (600 MHz, DMSO-*d*₆) δ 8.24 (t, *J* = 6 Hz, 2H), 7.92 (d, *J* = 3.6 Hz, 2H), 7.26 (s, 4H), 4.50 (d, *J* = 6 Hz, 4H), 3.72 (s, 6H). ¹³C NMR (150 MHz, DMSO-*d*₆) δ 160.49, 153.21, 143.34, 139.00, 137.82, 127.31, 54.23, 42.78. HRMS calcd for C₁₈H₁₉F₂N₆O₂ 389.15376 [M + H]⁺, found 389.15330. Anal. (C₁₈H₁₈F₂N₆O₂) C, H, N.

***N*-(4-((5-Fluoropyrimidin-2-ylamino)methyl)benzyl)-4-(trifluoromethyl)pyrimidin-2-amine (21a)**. To a solution of mono boc-protected 1,4-phenylenedimethanamine **19** (11.80 g, 50 mmol) in DMF (50 mL) was added 2-chloro-5-fluoropyrimidine (7.29 g, 55 mmol) and *N,N*-diisopropylethylamine (30.5 mL, 175 mmol) at room temperature. The resulting mixture was heated to 60 °C and stirred until the starting material disappeared from TLC plate. The reaction mixture was cooled down to ambient temperature, poured into ice water (200 mL), and extracted with ethyl acetate (3 × 50 mL). The combined organic layers were washed with brine, dried over anhydrous MgSO₄, and concentrated in vacuo. The crude was purified by flash column chromatography (silica gel, MeOH/CH₂Cl₂, 0 → 20%) to give the intermediate **19a** (4.25 g, 23%) as a white solid. ¹H NMR (600 MHz, CDCl₃) δ 8.15 (s, 2H), 7.30 (d, *J* = 6 Hz, 2H), 7.25 (d, *J* = 7.8 Hz, 2H), 5.57 (bs, 1H), 4.87 (bs, 1H), 4.57 (d, *J* = 5.4 Hz, 2H), 4.30 (d, *J* = 5.4 Hz, 2H), 1.46 (s, 9H). ¹³C NMR (600 MHz, CDCl₃) δ 159.43, 156.08, 153.23, 151.59, 145.76 (d, *J* = 85.2 Hz), 138.27, 127.98, 127.90, 79.73, 45.89, 44.56, 28.61. HRMS Calcd for C₁₇H₂₁FN₄O₂ 333.16485 [M + H]⁺, found 333.17232.

To a solution of the intermediate **19a** (1.66 g, 5.0 mmol) in methanol (15 mL) was added thionyl chloride (0.73 mL, 10.0 mmol) dropwise at 0 °C. The resulting mixture was warmed to ambient temperature and stirred until complete consumption of the starting material from TLC plate. The reaction mixture was diluted with diethyl ether (150 mL). The off-white solid was collected, washed with diethyl ether, dried under vacuum, and used in the next step without further purification. The crude solid obtained as above was dissolved in DMF (15 mL), to which was added 2-chloro-4-(trifluoromethyl)pyrimidine (1.03 g, 5.5 mmol) and *N,N*-diisopropylethylamine (4.4 mL, 25 mmol) at room temperature. The resulting mixture was heated to 90 °C and stirred until the starting material disappeared from TLC plate. The reaction mixture was cooled down to ambient temperature, poured into ice water (60 mL), and extracted with ethyl acetate (3 × 15 mL). The combined organic layers were washed with brine, dried over anhydrous MgSO₄, and concentrated in vacuo. The crude was purified by flash column chromatography (silica gel, MeOH/CH₂Cl₂, 0 → 20%) to give the intermediate **21a** (1.27 g, 67%) as a white solid: mp 164–165 °C (dec). ¹H NMR (600 MHz, DMSO-*d*₆) δ 8.57 (d, *J* = 4.2 Hz, 1H), 8.42 (bs, 1H), 8.32 (s, 2H), 7.76 (t, *J* = 6 Hz, 1H), 7.23 (m, 4H), 6.96 (d, *J* = 5.4 Hz, 1H), 4.49 (bs, 1H), 4.44 (bs, 1H), 4.41 (d, *J* = 6 Hz, 2H). ¹³C NMR (150 MHz, DMSO-*d*₆) δ 162.21, 161.47, 159.48, 152.43, 150.81, 145.58, 138.68, 137.78, 127.42, 126.92, 121.58, 104.87, 44.24, 43.75. HRMS calcd for C₁₇H₁₅F₄N₆ 379.12943 [M + H]⁺, found 379.12905. Anal. (C₁₇H₁₄F₄N₆) C, H, N.

5-Fluoro-*N*-(4-((2-(methylthio)pyrimidin-4-ylamino)methyl)benzyl)pyrimidin-2-amine (21b). Starting with compound **19a** (1.66 g, 5.0 mmol), the same procedure as that for compound **21a** furnished the title product **21b** (1.19 g, 67%) as a white solid: mp 162–163 °C (dec). ¹H NMR (600 MHz, DMSO-*d*₆) δ 8.16 (s, 2H), 7.99 (d, *J* = 3 Hz, 1H), 7.30 (m, 4H), 6.01 (m, 1H), 5.55 (bs, 1H), 5.24 (bs, 1H), 4.59 (m, 2H), 4.54 (bs, 2H), 2.49 (s, 3H). ¹³C NMR (150 MHz, DMSO-*d*₆) δ 171.90, 159.44, 155.70, 153.29, 151.64, 145.86, 145.71, 138.74, 137.23, 128.04, 100.00, 45.83, 45.16, 14.16. HRMS calcd for C₁₇H₁₈FN₆S 357.12977 [M + H]⁺, found 357.12931. Anal. (C₁₇H₁₇FN₆S) C, H, N.

(4-(2-Ethoxyethyl)piperazin-1-yl)(2-(4-((5-fluoropyrimidin-2-ylamino)methyl)benzylamino)-4-(trifluoromethyl)pyrimidin-5-yl)-methanone (21c). Starting with compound **19a** (1.66 g, 5.0 mmol), the same procedure as for that of compound **21c** furnished the title product **21c** (1.77 g, 63%) as a white solid: mp 158–159 °C.

^1H NMR (600 MHz, CDCl_3) δ 8.18 (s, 2H), 7.32 (s, 4H), 7.27 (s, 1H), 5.94 (bs, 1H), 5.48 (bs, 1H), 4.65 (s, 2H), 4.60 (d, $J = 6$ Hz, 2H), 3.80 (d, $J = 22.2$ Hz, 2H), 3.56 (t, $J = 6$ Hz, 2H), 3.50 (dd, $J = 7.2$ Hz, 2H), 3.33 (s, 2H), 2.63 (t, $J = 5.4$ Hz, 2H), 2.58 (s, 2H), 2.46 (bs, 2H), 1.20 (t, $J = 7.2$ Hz, 3H). ^{13}C NMR (150 MHz, $\text{DMSO}-d_6$) δ 163.50, 161.39, 159.49, 159.11, 152.44, 150.83, 145.64, 138.79, 137.42, 127.51, 126.98, 115.88, 67.69, 65.45, 57.02, 52.91, 52.51, 46.85, 44.24, 43.82, 41.42. HRMS calcd for $\text{C}_{26}\text{H}_{29}\text{F}_4\text{N}_8\text{O}_2$ 563.25061 [$\text{M} + \text{H}$] $^+$, found 563.24907. Anal. ($\text{C}_{26}\text{H}_{30}\text{F}_4\text{N}_8\text{O}_2$) C, H, N.

tert-Butyl 4-((2-Chloro-5-fluoropyrimidin-4-ylamino)methyl)benzylcarbamate (23). To a mixture of mono boc-protected 1,4-phenylenedimethanamine **19** (20.0 g, 80 mmol), *N,N'*-diisopropylethylamine (52 mL, 300 mmol) in DMF (200 mL) was slowly added 2,4-dichloro-5-fluoropyrimidine (14.9 g, 89 mmol). The resulting mixture was heated to 60 °C and stirred for 1 h. TLC indicated complete consumption of the starting material. The reaction was cooled to ambient temperature, poured into ice water (800 mL), and extracted with ethyl acetate (3 \times 150 mL). The combined organic layers were washed with brine, dried over anhydrous MgSO_4 , and concentrated in vacuo. The crude was purified by flash column chromatography (silica gel, $\text{MeOH}/\text{CH}_2\text{Cl}_2$, 0 \rightarrow 20%) to give the title compound **23** (29.1 g, 94%) as a white solid: mp 127 °C (dec). ^1H NMR (600 MHz, CDCl_3) δ 7.89 (d, $J = 3$ Hz, 1H), 7.31–7.27 (m, 4H), 5.51 (s, 1H), 4.49 (s, 1H), 4.66 (d, $J = 5.4$ Hz, 2H), 4.31 (d, $J = 6$ Hz, 2H), 1.45 (s, 9H). ^{13}C NMR (150 MHz, $\text{DMSO}-d_6$) δ 156.10, 153.59, 146.25, 144.55, 140.09, 140.02, 139.20, 136.26, 128.59, 128.13, 79.84, 44.71, 44.47, 28.60. HRMS calcd for $\text{C}_{17}\text{H}_{21}\text{ClFN}_4\text{O}_2$ 367.13371 [$\text{M} + \text{H}$] $^+$, found 367.13325.

2-Chloro-5-fluoro-*N*-(4-((2-(methylthio)pyrimidin-4-ylamino)methyl)benzyl)pyrimidin-4-amine (24). Thionyl chloride (11.62 mL, 160 mmol) was added dropwise to a solution of compound **19** (29.1 g, 80 mmol) in methanol (300 mL) at 0 °C. The resulting mixture was warmed to ambient temperature and stirred until complete consumption of the starting material was observed from the TLC plate. The reaction mixture was diluted with 700 mL of ether. The off-white solid was collected, washed with diethyl ether, dried under vacuum, and used in next step without further purification.

The crude solid obtained as above was dissolved in DMF (200 mL), to which was added 4-chloro-2-thiomethylpyrimidine (14.1 g, 88 mmol) and *N,N'*-diisopropylethylamine (59.2 mL, 340 mmol) at room temperature. The resulting mixture was heated to 90 °C and stirred until the starting material disappeared from TLC plate. The reaction mixture was cooled down to ambient temperature, poured into ice water (1.0 L), and extracted with ethyl acetate (3 \times 200 mL). The combined organic layers were washed with brine, dried over anhydrous MgSO_4 , and concentrated in vacuo. The crude was purified by flash column chromatography (silica gel, $\text{MeOH}/\text{CH}_2\text{Cl}_2$, 0 \rightarrow 20%) to give the desired product **24** (20.1 g, 66%, 2 steps) as a white solid. ^1H NMR (600 MHz, $\text{DMSO}-d_6$) δ 8.73 (t, $J = 5.4$ Hz, 1H), 8.09 (d, $J = 3.6$ Hz, 1H), 7.95 (t, $J = 6$ Hz, 1H), 7.86 (bs, 1H), 7.27 (s, 4H), 6.22 (s, 1H), 4.53 (d, $J = 60$ Hz, 2H), 4.49 (bs, 2H), 2.36 (s, 3H). ^{13}C NMR (150 MHz, $\text{DMSO}-d_6$) δ 170.12, 160.67, 153.96, 153.43, 146.06, 144.37, 139.78, 138.30, 136.98, 127.41, 127.39, 101.92, 43.00, 39.92, 13.28. HRMS calcd for $\text{C}_{17}\text{H}_{17}\text{ClFN}_6\text{S}$ 391.09080 [$\text{M} + \text{H}$] $^+$, found 391.09050.

Preparation of Compound 26. To a mixture of compound **24** (5.0 g, 12.8 mmol) in methylene chloride (50 mL) was added 3-chloroperoxybenzoic acid (3.3 g, 19.2 mmol) at a rate to maintain the temperature below 0 °C. The resulting mixture was stirred at that temperature until no more starting material was detected from TLC. The reaction then was quenched by the addition of saturated aqueous NaHCO_3 . After separation, the aqueous layer was extracted with additional methylene chloride (2 \times 20 mL). The combined organic layers were dried over MgSO_4 and concentrated under reduced pressure to afford a mixture of sulfoxide and sulfone as a yellow solid, which was used without additional purification.

The crude mixture obtained as above was dissolved in 1,4-dioxane (50 mL), to which *N,N'*-diisopropylethylamine (6.8 mL, 38.4 mmol) and 4-(2-aminoethyl)morpholine (2.0 g, 15.4 mmol) was added slowly. The resulting mixture was heated to 95 °C and stirred for 18 h. After cooling to ambient temperature, the reaction mixture was partitioned using ethyl acetate (100 mL) and saturated aqueous NaHCO_3 (100 mL). The aqueous layer was extracted with additional ethyl acetate (2 \times 20 mL). The combined organic layers were further washed with brine, dried over MgSO_4 , filtered, and concentrated under reduced pressure. The crude was purified by flash column chromatography (silica gel, $\text{MeOH}/\text{CH}_2\text{Cl}_2$, 0 \rightarrow 40%) to give the desired product **26** (1.5 g, 25%, 2 steps) as an off-white solid: mp 68 °C (dec). ^1H NMR (300 MHz, CDCl_3) δ 7.92 (d, $J = 2.7$ Hz, 1H), 7.85 (d, $J = 6.0$ Hz, 1H), 7.33 (s, 4H), 5.70 (d, $J = 5.4$ Hz, 1H), 5.51 (bs, 1H), 5.33 (bs, 1H), 4.97 (bs, 1H), 4.69 (d, $J = 5.7$ Hz, 2H), 4.54 (d, $J = 5.4$ Hz, 2H), 3.70 (t, $J = 4.5$ Hz, 4H), 3.45 (dd, $J = 5.7, 5.7$ Hz, 2H), 2.57–2.45 (m, 6H). ^{13}C NMR (150 MHz, $\text{DMSO}-d_6$) δ 162.23, 161.98, 153.42, 146.061, 144.360, 139.92, 139.78, 136.70, 127.31, 127.19, 66.19, 57.64, 53.34, 42.99, 40.04, 37.59. HRMS calcd for $\text{C}_{22}\text{H}_{27}\text{ClFN}_8\text{O}$ 473.19804 [$\text{M} + \text{H}$] $^+$, found 473.20026. Anal. ($\text{C}_{22}\text{H}_{26}\text{ClFN}_8\text{O}$) C, H, N.

Acknowledgment. This study was supported by Distinguished Cancer Scientist Development Fund of Georgia Cancer Coalition, and NCI R01 CA 109366 (H.S.) and NIH R01 CA126447 (H.E.G.). We are grateful to Jessica Paulishen for careful reading of the manuscript and helpful remarks.

Supporting Information Available: Elemental analysis of all final compounds. This material is available free of charge via the Internet at <http://pubs.acs.org>.

References

- Butcher, E. C.; Williams, M.; Youngman, K.; Rott, L.; Briskin, M. Lymphocyte trafficking and regional immunity. *Adv. Immunol.* **1999**, *72*, 209–253.
- Forster, R.; Schubel, A.; Breitfeld, D.; Kremmer, E.; Renner-Muller, I.; Wolf, E.; Lipp, M. CCR7 coordinates the primary immune response by establishing functional microenvironments in secondary lymphoid organs. *Cell* **1999**, *99*, 23–33.
- Peled, A.; Petit, I.; Kollet, O.; Magid, M.; Ponomaryov, T.; Byk, T.; Nagler, A.; Ben-Hur, H.; Many, A.; Shultz, L.; Lider, O.; Alon, R.; Zipori, D.; Lapidot, T. Dependence of human stem cell engraftment and repopulation of NOD/SCID mice on CXCR4. *Science* **1999**, *283*, 845–848.
- Davis, C. B.; Dikic, I.; Unutmaz, D.; Hill, C. M.; Arthos, J.; Siani, M. A.; Thompson, D. A.; Schlessinger, J.; Littman, D. R. Signal transduction due to HIV-1 envelope interactions with chemokine receptors CXCR4 or CCR5. *J. Exp. Med.* **1997**, *186*, 1793–1798.
- Zaitseva, M.; Blauvelt, A.; Lee, S.; Lapham, C. K.; Klaus-Kovtun, V.; Mostowski, H.; Manischewitz, J.; Golding, H. Expression and function of CCR5 and CXCR4 on human Langerhans cells and macrophages: implications for HIV primary infection. *Nature Med.* **1997**, *3*, 1369–1375.
- Sanchez, X.; Cousins-Hodges, B.; Aguilar, T.; Gosselink, P.; Lu, Z.; Navarro, J. Activation of HIV-1 coreceptor (CXCR4) mediates myelosuppression. *J. Biol. Chem.* **1997**, *272*, 27529–27531.
- Feng, Y.; Broder, C. C.; Kennedy, P. E.; Berger, E. A. HIV-1 entry cofactor: functional cDNA cloning of a seven-transmembrane, G protein-coupled receptor. *Science* **1996**, *272*, 872–877.
- De Clercq, E. The bicyclam AMD3100 story. *Nature Rev. Drug Discovery* **2003**, *2*, 581–587.
- Zhan, W.; Liang, Z.; Zhu, A.; Kurtkaya, S.; Shim, H.; Snyder, J. P.; Liotta, D. C. Discovery of small molecule CXCR4 antagonists. *J. Med. Chem.* **2007**, *50*, 5655–5664.
- Fujii, N.; Tamamura, H. Peptide-lead CXCR4 antagonists with high anti-HIV activity. *Curr. Opin. Invest. Drugs* **2001**, *2*, 1198–1202.
- Liang, Z.; Wu, T.; Lou, H.; Yu, X.; Taichman, R. S.; Lau, S. K.; Nie, S.; Umbreit, J.; Shim, H. Inhibition of breast cancer metastasis by selective synthetic polypeptide against CXCR4. *Cancer Res.* **2004**, *64*, 4302–4308.
- Onuffer, J. J.; Horuk, R. Chemokines, chemokine receptors and small-molecule antagonists: recent developments. *Trends Pharmacol. Sci.* **2002**, *23*, 459–467.

- (13) Donzella, G. A.; Schols, D.; Lin, S. W.; Este, J. A.; Nagashima, K. A.; Maddon, P. J.; Allaway, G. P.; Sakmar, T. P.; Henson, G.; De Clercq, E.; Moore, J. P. AMD3100, a small molecule inhibitor of HIV-1 entry via the CXCR4 co-receptor. *Nature Med.* **1998**, *4*, 72–77.
- (14) Fujii, N.; Nakashima, H.; Tamamura, H. The therapeutic potential of CXCR4 antagonists in the treatment of HIV. *Expert Opin. Invest. Drugs* **2003**, *12*, 185–195.
- (15) Abdel-Magid, A. F.; Carson, K. G.; Harris, B. D.; Maryanoff, C. A.; Shah, R. D. Reductive Amination of Aldehydes and Ketones with Sodium Triacetoxyborohydride. Studies on Direct and Indirect Reductive Amination Procedures. *J. Org. Chem.* **1996**, *61*, 3849–3862.
- (16) Liang, Z.; Brooks, J.; Willard, M.; Liang, K.; Yoon, Y.; Kang, S.; Shim, H. CXCR4/CXCL12 axis promotes VEGF-mediated tumor angiogenesis through Akt signaling pathway. *Biochem. Biophys. Res. Commun.* **2007**, *359*, 716–722.
- (17) Chavance, M.; Escolano, S.; Romon, M.; Basdevant, A.; de Lauzon-Guillain, B.; Charles, M. A. Latent variables and structural equation models for longitudinal relationships: an illustration in nutritional epidemiology. *BMC Med. Res. Methodol.* **2010**, *10*, 37.
- (18) Xu, J.; Mora, A.; Shim, H.; Stecenko, A.; Brigham, K. L.; Rojas, M. Role of the SDF-1/CXCR4 axis in the pathogenesis of lung injury and fibrosis. *Am. J. Respir. Cell Mol. Biol.* **2007**, *37*, 291–299.
- (19) Hashimoto, N.; Jin, H.; Liu, T.; Chensue, S. W.; Phan, S. H. Bone marrow-derived progenitor cells in pulmonary fibrosis. *J. Clin. Invest.* **2004**, *113*, 243–252.
- (20) Yang, H.; Grossniklaus, H. E. Combined immunologic and anti-angiogenic therapy reduces hepatic micrometastases in a murine ocular melanoma model. *Curr. Eye Res.* **2006**, *31*, 557–562.
- (21) Yang, J.; Zhang, B.; Lin, Y.; Yang, Y.; Liu, X.; Lu, F. Breast cancer metastasis suppressor 1 inhibits SDF-1 α -induced migration of non-small cell lung cancer by decreasing CXCR4 expression. *Cancer Lett.* **2008**, *269*, 46–56.
- (22) Dithmar, S.; Rusciano, D.; Grossniklaus, H. E. A new technique for implantation of tissue culture melanoma cells in a murine model of metastatic ocular melanoma. *Melanoma Res.* **2000**, *10*, 2–8.
- (23) Trent, J. O.; Wang, Z. X.; Murray, J. L.; Shao, W.; Tamamura, H.; Fujii, N.; Peiper, S. C. Lipid bilayer simulations of CXCR4 with inverse agonists and weak partial agonists. *J. Biol. Chem.* **2003**, *278*, 47136–47144.
- (24) Mori, T.; Doi, R.; Koizumi, M.; Toyoda, E.; Ito, D.; Kami, K.; Masui, T.; Fujimoto, K.; Tamamura, H.; Hiramatsu, K.; Fujii, N.; Imamura, M. CXCR4 antagonist inhibits stromal cell-derived factor 1-induced migration and invasion of human pancreatic cancer. *Mol. Cancer Ther.* **2004**, *3*, 29–37.
- (25) Oonuma, T.; Morimatsu, M.; Nakagawa, T.; Uyama, R.; Sasaki, N.; Nakaichi, M.; Tamamura, H.; Fujii, N.; Hashimoto, S.; Yamamura, H.; Syuto, B. Role of CXCR4 and SDF-1 in mammary tumor metastasis in the cat. *J. Vet. Med. Sci.* **2003**, *65*, 1069–1073.
- (26) Tamamura, H.; Hori, A.; Kanzaki, N.; Hiramatsu, K.; Mizumoto, M.; Nakashima, H.; Yamamoto, N.; Otaka, A.; Fujii, N. T140 analogs as CXCR4 antagonists identified as anti-metastatic agents in the treatment of breast cancer. *FEBS Lett.* **2003**, *550*, 79–83.
- (27) Hatse, S.; Princen, K.; Bridger, G.; De Clercq, E.; Schols, D. Chemokine receptor inhibition by AMD3100 is strictly confined to CXCR4. *FEBS Lett.* **2002**, *527*, 255–262.
- (28) Schols, D.; Este, J. A.; Henson, G.; De Clercq, E. Bicyclams, a class of potent anti-HIV agents, are targeted at the HIV coreceptor fusin/CXCR-4. *Antiviral Res.* **1997**, *35*, 147–156.
- (29) Dorsam, R. T.; Gutkind, J. S. G-protein-coupled receptors and cancer. *Nature Rev. Cancer* **2007**, *7*, 79–94.
- (30) Richard, C. L.; Blay, J. CXCR4 in Cancer and Its Regulation by PPAR γ . *PPAR Res* **2008**, *2008*, 769413.
- (31) Zhu, A.; Yoon, Y.; Voll, R.; Williams, L.; Liang, Z.; Camp, V.; Liotta, D.; Goodman, M.; Shim, H. In SNM 57th Annual Meeting, Salt Lake City, Utah, 2010.
- (32) Gupta, S. K.; Pillarisetti, K.; Thomas, R. A.; Aiyar, N. Pharmacological evidence for complex and multiple site interaction of CXCR4 with SDF-1 α : implications for development of selective CXCR4 antagonists. *Immunol. Lett.* **2001**, *78*, 29–34.
- (33) Pyo, R. T.; Sui, J.; Dhume, A.; Palomeque, J.; Blaxall, B. C.; Diaz, G.; Tunstead, J.; Logothetis, D. E.; Hajjar, R. J.; Schecter, A. D. CXCR4 modulates contractility in adult cardiac myocytes. *J. Mol. Cell. Cardiol.* **2006**, *41*, 834–844.
- (34) Gao, C.; Li, Y. SDF-1 plays a key role in the repairing and remodeling process on rat allo-orthotopic abdominal aorta grafts. *Transplant Proc.* **2007**, *39*, 268–272.
- (35) Imitola, J.; Raddassi, K.; Park, K. I.; Mueller, F. J.; Nieto, M.; Teng, Y. D.; Frenkel, D.; Li, J.; Sidman, R. L.; Walsh, C. A.; Snyder, E. Y.; Khoury, S. J. Directed migration of neural stem cells to sites of CNS injury by the stromal cell-derived factor 1 α /CXCR4 chemokine receptor 4 pathway. *Proc. Natl. Acad. Sci. U.S.A.* **2004**, *101*, 18117–18122.
- (36) Kajiyama, H.; Shibata, K.; Ino, K.; Nawa, A.; Mizutani, S.; Kikkawa, F. Possible involvement of SDF-1 α /CXCR4-DPP4 axis in TGF- β 1-induced enhancement of migratory potential in human peritoneal mesothelial cells. *Cell Tissue Res.* **2007**, *330*, 221–229.
- (37) Moyer, R. A.; Wendt, M. K.; Johanesen, P. A.; Turner, J. R.; Dwinell, M. B. Rho activation regulates CXCL12 chemokine stimulated actin rearrangement and restitution in model intestinal epithelia. *Lab. Invest.* **2007**, *87*, 807–817.
- (38) Liang, Z.; Yoon, Y.; Votaw, J.; Goodman, M. M.; Williams, L.; Shim, H. Silencing of CXCR4 blocks breast cancer metastasis. *Cancer Res.* **2005**, *65*, 967–971.
- (39) Yoon, Y.; Liang, Z.; Zhang, X.; Choe, M.; Zhu, A.; Cho, H. T.; Shin, D. M.; Goodman, M. M.; Chen, Z. G.; Shim, H. CXCR4 chemokine receptor-4 antagonist blocks both growth of primary tumor and metastasis of head and neck cancer in xenograft mouse models. *Cancer Res.* **2007**, *67*, 7518–7524.